Inorg. Chem. **2008**, *47*, 9745−9747

Inorganic Chemistry
Communication

Magnetic Spongelike Behavior of 3D Ferrimagnetic $\{[Mn^{II}(imH)]_2[Nb^{IV}(CN)_8]\}_n$ with $T_c = 62$ K

Dawid Pinkowicz,*,[†] Robert Podgajny,*,[†] Maria Bałanda,[‡] Magdalena Makarewicz,[‡] Bartłomiej Gaweł,[†] Wiesław Łasocha,[†] and Barbara Sieklucka[†]

Faculty of Chemistry, Jagiellonian University, Ingardena 3, 30-060 Kraków, Poland, and H. Niewodniczański Institute of Nuclear Physics PAN, Radzikowskiego 152, 31-342 Kraków, Poland

Received July 8, 2008

Fully reversible room temperature dehydration of 3D $\{Mn^{II}_2(imH)_2(H_2O)_4[Nb^{IV}(CN)_8]\cdot 4H_2O\}_n$ (**1**; imH = imidazole) of T_c = 25 K results in the formation of 3D ferrimagnet $\{[Mn^{II}(imH)]_2[Nb^{IV}(CN)_8]\}_n$ (**2**), with T_c = 62 K, the highest ever known for octacyanometalate-based compounds. The dramatic magnetostructural modifications in **2** provide the first example of magnetic spongelike behavior in an octacyanometallate-based assembly.

A strong current motivation for the synthesis of heterometallic inorganic−organic hybrid materials incorporating paramagnetic $[M(CN)_8]^{n-}$ (M = Nb^{IV}, Mo^{V}, W^{V}) ions is the merging of multifunctionality into these systems. Engineering of these materials by selecting the appropriate paramagnetic octacyanometalate building block, 3d metal ion, and organic ligands is the key to understanding of possible synergies between magnetic coupling and magnetic ordering T_c and the physicochemical properties associated with their often porous nature, guest sorption/desorption, optical metal-to-metal charge transfer, and physically or chemically modulated structural and/or interstate equilibria.

The investigation of high-T_c octacyanometalate-based molecular magnets led to the construction of a series of simple bimetallic as well as hybrid 2D and 3D cyano-bridged $[M^{V}(CN)_8]^{3-}$ 3d−4f metal (M = Mo, W) networks with critical temperature T_c values not exceeding 54 K.[1−4] The $[Nb^{IV}(CN)_8]^{4-}$ building block has been very scarcely used in the construction of magnetic networks in comparison to its $[W^{V}(CN)_8]^{3-}$ and $[Mo^{V}(CN)_8]^{3-}$ analogues. Relatively strong antiferromagnetic 3d metal−NC−Nb^{IV} exchange led to long-range magnetic ordering below T_c = 51 K for 3D ferrimagnet $\{Mn^{II}_2(H_2O)_4[Nb^{IV}(CN)_8]\cdot 4H_2O\}$ (**1**)[3a] as well as to a high-spin ground state in the case of the discrete assemblies,[5] with *J* values being representative for this class of compounds.[6] Our pioneering investigations into $Mn^{II}_2Nb^{IV}$ inorganic−organic hybrid networks have already afforded the series of 3D soft ferrimagnetic $Mn^{II}L[Nb^{IV}(CN)_8]^{4-}$ compounds (L = pz, pyrazine; pzdo, pyrazine di-*N*,*N*′-oxide; bpym, bipyrimidine) exhibiting long-range ordering with T_c values in the range 27−50 K.[7a] Very recently, we reported on the synthesis and magnetic properties of $\{Mn^{II}_2(imH)_2(H_2O)_4[Nb^{IV}(CN)_8]\cdot 4H_2O\}_n$ **1**, with imidazole (imH) molecules acting as monodentate ligands.[7b] The 3D cyano-bridged coordination framework of **1** is made of two groups of mutually parallel 1D ladders cross-linked at Nb centers (Figure 1, left). Coordination spheres of both Mn ions in **1** are pseudo-octahedral with three nitrogen atoms of bridging cyanides, two oxygen atoms of the coordination water, and one nitrogen of the monodentate imidazole ligand. The dodecahedral coordination sphere of Nb contains two terminal and six bridging cyano ligands. Magnetic measurements revealed that **1** is a soft ferrimagnet with T_c of 25 K. Herein, we present a novel compound $\{[Mn^{II}(imH)]_2[Nb^{IV}(CN)_8]\}_n$ (**2**), which can be obtained from **1** by controlled thermal treatment in the atmosphere

---

* To whom correspondence should be addressed. E-mail: pinkowic@chemia.uj.edu.pl (D.P.), podgajny@chemia.uj.edu.pl (R.P.).

[†] Jagiellonian University.

[‡] H. Niewodniczański Institute of Nuclear Physics PAN.

(1) Sieklucka, B.; Podgajny, R.; Przychodzeń, P.; Korzeniak, T. *Coord. Chem. Rev.* **2005**, *249*, 2203–2221.

(2) Przychodzeń, P.; Korzeniak, T.; Podgajny, R.; Sieklucka, B. *Coord. Chem. Rev.* **2006**, *250*, 2234–2260.

(3) (a) Pilkington, M.; Decurtins, S. *Chimia* **2000**, *54*, 593–601. (b) Zhong, Z. J.; Seino, H.; Mizobe, Y.; Hidai, M.; Verdaguer, M.; Ohkoshi, S.-i.; Hashimoto, K. *Inorg. Chem.* **2000**, *39*, 5095–5101. (c) Kashigawi, T.; Ohkoshi, S.-i.; Seino, H.; Mizobe, Y.; Hashimoto, K. *J. Am. Chem. Soc.* **2004**, *126*, 5024–5025. (d) Chibotaru, L. F.; Mironov, V. S.; Ceulemans, A. *Angew. Chem., Int. Ed.* **2001**, *40*, 4429–4433.

(4) Withers, J. R.; Li, D.; Triplet, J.; Ruschman, Ch.; Parkin, S.; Wang, G.; Yee, G. T.; Holmes, St. *Inorg. Chem.* **2006**, *45*, 4307.

(5) Venktakrishnan, Th. S.; Rajamani, R.; Ramasesha, S.; Sutter, J.-P. *Inorg. Chem.* **2007**, *46*, 9569–9574.

(6) (a) Podgajny, R.; Desplanches, C.; Sieklucka, B.; Villar, V.; Paulsen, C.; Wernsdorfer, W.; Dromzee, Y.; Verdaguer, M. *Inorg. Chem.* **2002**, *41*, 1323–1327. (b) Zhao, H.; Shatruk, M.; Prosvirin, A. V.; Dunbar, K. R. *Chem.*−*Eur. J.* **2007**, *13*, 6573–6589. (c) Ruiz, E.; Rajaraman, G.; Alvarez, S.; Gillon, B.; Stride, J.; Clérac, R.; Larionova, J.; Descurtins, S. *Angew. Chem., Int. Ed.* **2005**, *44*, 2711–2715. (d) Wang, Zh.-X.; Li, X.-L.; Wang, T.-W.; Li, Y.-Zh.; Ohkoshi, S.-i.; Hashimoto, K.; Song, Y.; You, X.-Z. *Inorg. Chem.* **2007**, *46*, 10990–10995.

(7) (a) Podgajny, R.; Pinkowicz, D.; Korzeniak, T.; Nitek, W.; Rams, M.; Sieklucka, B. *Inorg. Chem.* **2007**, *46*, 10416. (b) Pinkowicz, D.; Podgajny, R.; Nitek, W.; Makarewicz, M.; Czapla, M.; Mihalik, M.; Bałanda, M.; Sieklucka, B. *Inorg. Chim. Acta* **2008**, *361*, 3957–3962.

10.1021/ic801248f CCC: $40.75

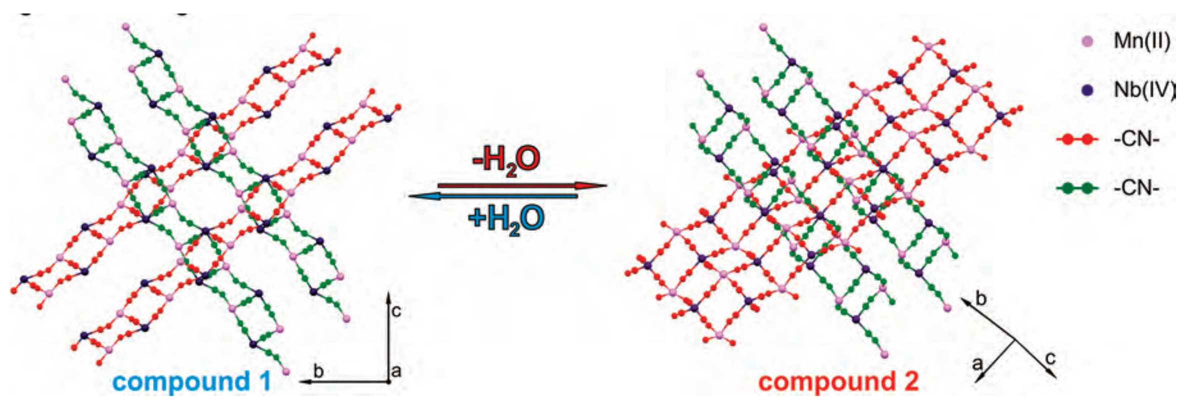

Figure 1. Cyano-bridged frameworks of **1** and **2**. Reversible changes in the cyano-bridged framework are caused by dehydration/rehydration processes (imidazole, H_2O molecules, and terminal cyanide ligands are omitted for clarity).

of argon[8] or by drying over phosphorus(V) oxide under reduced pressure of argon in ambient temperature.[9]

Powder X-ray diffraction (PXRD) analysis[10] revealed the network of **2** consisting of Mn1−Nb1 square-grid motifs cross-linked at Nb1 centers by 1D Mn2−Nb1 ladders (Figure S1 in the Supporting Information (SI) and Figure 1, right). Table S1 in the SI shows the established values of metric parameters for **2**. Figures S2 and S3 in the SI show the atom-labeling scheme, coordination environment, and overall connectivity of a cyano-bridged network. Within a 5.6 Å distance from Nb, which is the average length of a Nb−CN−Mn linkage,[3a,7a] seven manganese centers are present, indicating the formation of seven CN^- bridges toward neighboring Mn^{II} (Figure S3a in the SI). The most important features of the two types of Mn^{II} centers present are their reduced coordination numbers. Mn1, which forms exclusively square-grid motifs, has a distorted trigonal-bipyramidal geometry with four nitrogen atoms of cyanides and one nitrogen of the imidazole ligand in its coordination sphere (Figure S3b in the SI). The Mn2 center, forming ladder motifs, coordinates three nitrogen atoms of cyanide and one nitrogen atom of imidazole in a distorted tetrahedral geometry (Figure S3c in the SI). The structural model of **2** reveals significant changes made to the 3D framework of **1** by release of H_2O molecules (Figure 1). The cyano-bridged network of **2** resembles the parent one, with one set of ladders transformed into square grids.

Figure S4 in the SI presents in detail reversible structural modifications between **1** and **2**. We have found that the formation of the seventh Nb1−CN−Mn1 linkage in **2** occurs as a consequence of breaking of the clearly defined and well-situated hydrogen-bonding system in **1**. This involves one of the terminal CN^- ligands, crystallization H_2O, and coordination H_2O molecules arranged in a hexagonal pattern within the cavity surrounded by the ladders in the parent cyano-bridged framework. The removal of all H_2O molecules provokes a closer approach of the CN^- ligand to the Mn and, finally, formation of the novel Nb1−CN−Mn1 linkage. The structure of **2** is very efficiently stabilized by relatively strong $\pi-\pi$ stacking of imidazole rings (arranged in quaternary arrays) with an average distance of 3.5 Å within the array (Figure S5 in the SI), favored in the case of the absence of hydrogen bonding involving H_2O. Reversibility of the transformation was confirmed by elemental analysis, IR spectroscopy,[11] and magnetic measurements.

The IR spectrum (Figure S6 in the SI) of **2** in the range of ν(CN) shows two strong bands, 2151 and 2141 cm^{-1}, characteristic of the bridging mode of CN^- ligands. In comparison to **1**, a dramatic decrease in the intensity at 2111

---

(8) Thermogravimetric quadrupole mass spectrometry measurements for **2** revealed a stepwise weight loss. The first step with a maximum at 90 °C corresponds to the loss of both solvate and coordination H_2O ($q/m = 18^+$). The second step occurring above 200 °C is assigned to the loss of cyanide ligands (lines $q/m = 26^+$ and 27^+) and is associated with collective decomposition of the compound.

(9) A freshly prepared powdered sample of **2** (0.54 mmol, 370.9 mg) was placed over phosphorus(V) oxide under reduced pressure of argon in ambient temperature for 24 h. After this time, a weight loss of 74.1 mg corresponding to the release of eight H_2O molecules per formula unit of **2** was observed. The resulting red powder of **1** (0.54 mmol, 297.0 mg) was stored under argon in a desiccator. Yield: 100%. Anal. Calcd for $C_{14}H_8Mn_2N_{12}Nb$: C, 30.7; H, 1.5; N, 30.7. Found: C, 30.6; H, 1.4; N, 30.25. IR (Nujol, cm^{-1}): ν_{N-H} 3422 s, $\nu_{C\equiv N}$ 2151 vs, $\nu_{C\equiv N}$ 2140 vs, imidazole I band 1620 vw, $\nu_{C=N}$ 1540 m, $\nu_{C=C}$ 1502 m, δ_{imH} 1328 m, δ_{imH} 1306 w, δ_{imH} 1268 w, δ_{imH} 1195 vw, δ_{imH} 1164 vw, δ_{imH} 1145 vw, δ_{imH} 1107 vw, δ_{imH} 1097 vw, δ_{imH} 1078 m, δ_{imH} 1066s, 954 w, 942 w, 919 vw, 890 vw, 835 m, 791 w, 760 m, 723 m, 660 w, 638 w, 600 m, 490 m, 463 m, 410 w.

(10) PXRD measurements were performed on a Philips X'Pert Pro diffractometer with a Bragg−Brentano geometry using Cu Kα radiation ($\lambda = 1.541\,78$ Å). The patterns were collected at 298 K in the 5−80° 2θ angle range. The powder diffraction pattern (Figure S7 in the SI) was indexed using the PROSZKI package (space group $P\bar{1}$; $a = 10.139(2)$ Å, $b = 10.999(2)$ Å, $c = 9.989(2)$ Å, $\alpha = 104.11(1)°$, $\beta = 103.06(1)°$, $\gamma = 95.81(1)°$, $V = 1037.9(4)$ Å^3, $F_{20} = 15$). The obtained parameters were refined by fitting to the experimental pattern according to the LeBail method. The structure was solved by the direct-space parallel-tempering method using *FOX* software. The starting model consisted of one $[Nb^{IV}(CN)_8]^{4-}$ and two $[Mn(imH)]^{2+}$ moieties, with bonds distances and angles according to the Cambridge Structural Database. Optimization was carried out in a "relaxed mode of the flexibility model". The obtained structure model was refined by the Rietveld method using the *JANA2000* software. The final agreement factors are $R_p = 0.0451$ and $R_{wp} = 0.0593$. Because of the instability of the refinement, only rigid-body refinement of the above-presented moieties, as found by the *FOX* program, was performed. This procedure generates some errors in the bond distances and angles, noticeably larger compared to traditionally refined structures. However, the result of the fitting indicates that the framework of the structure is essentially correct with acceptable precision.

(11) A sample of **2** was placed over argon in a closed vessel filled with water vapor at room temperature. Within 2 h, a color change from red to pale yellow was observed. Anal. Calcd for $C_{14}H_{24}Mn_2N_{12}NbO_8$: C, 24.7; H, 3.1; N, 24.3. Found: C, 24.3; H, 3.5; N, 24.3. IR (KBr, cm^{-1}): ν_{O-H} 3566 br, ν_{N-H} 3429 s, ν_{C-H} 3123 s, $\nu_{C\equiv N}$ 2144 vs, $\nu_{C\equiv N}$ 2112 vs, δ_{O-H} 1634 s, $\nu_{C=N}$ 1539 m, $\nu_{C=C}$ 1506 w, δ_{imH} 1427 w, δ_{imH} 1326 w, δ_{imH} 1259 vw, δ_{imH} 1174 vw, δ_{imH} 1126 vw, δ_{imH} 1098 w, δ_{imH} 1066 s, 939 w, 921 vw, 845 w, 759 m, 649 s, 617 m, 602 s, 471 s, 451 s.

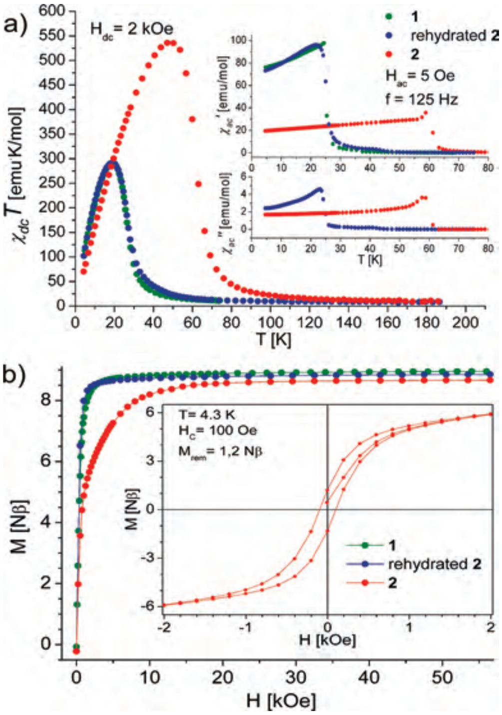

Figure 2. (a) $\chi_{dc}T(T)$, $\chi'_{ac}(T)$, and $\chi''_{ac}(T)$ (inset) dependences for **1** (green), **2** (red), and rehydrated **2** (blue). (b) $M(H)$ dependences for **1** (green), **2** (red), and rehydrated **2** (blue) and the magnetic hysteresis loop for **2** (inset).

cm^{-1} and a simultaneous increase at 2151 cm^{-1} confirm a change in the bridging mode of at least one terminal cyanide ligand. We observe also a complete decrease in the intensity of the band characteristic for the presence of H_2O molecules, particularly that of 1633 cm^{-1}, and the disappearance of the broad band in the region of 3600−3200 cm^{-1}, which is generally assigned to the strong hydrogen bonding (in this region, only a sharp band of the N−H stretching vibration remains). The IR spectrum of rehydrated **2** is almost identical with that of **1** (Figure S6 in the SI).

The temperature dependences of $\chi_{dc}T$, χ'_{ac}, and χ''_{ac} for **2** in the temperature range 4−190 K are given in Figure 2a, together with the magnetic characteristics obtained for **1** and rehydrated **2**. Upon cooling from 190 to 75 K, $\chi_{dc}T$, χ'_{ac}, and χ''_{ac} change very slowly. When the temperature reaches a value of about 70 K, the increase of $\chi_{dc}T$, χ'_{ac}, and χ''_{ac} for **2** becomes faster, and at T_c of 62 K, the abrupt increase of the magnetic response is observed, indicating unambiguously strong 3D magnetic ordering below this temperature. Fitting of the Curie−Weiss law to the data in the 90−190 K range gives $C = 6.9$ cm^3 K mol^{-1} and $\theta_{CW} = 69.4$ K, compared to $C = 6.8$ cm^3 K mol^{-1} and $\theta_{CW} = 32$ K for **1**.[7b] The high-temperature limit $\chi_M T$ of 8.14 cm^3 K mol^{-1} for **2** is lower than 9.125 cm^3 K mol^{-1} expected for two high-spin Mn^{II} ions ($S = {}^5/_2$) and one Nb^{IV} ion ($S = {}^1/_2$) assuming $g = 2$. The magnetization value at the field of 56 kOe measured at $T = 4.3$ K for **2** reaches the value of 8.7 Nβ, which is very close to the expected 9 Nβ (Figure 2b). **2** reveals a weak magnetic anisotropy, reflected in the slower magnetization $M(H)$ increase for **1** and in the hysteresis curve with a coercivity field of 100 Oe.

$\chi_{dc}T(T)$ and $\chi'_{ac}(T)$ dependences for both rehydrated **2** and substrate **1** are shown to be identical (Figure 2a). The sharp rise of $\chi_{dc}T(T)$ for rehydrated **2** at T_c of 25 K with a maximum of 291.9 emu K mol^{-1} at $T = 19.0$ K (applied field of 2 kOe) corresponds well to T_c of 25 K and $(\chi_{dc}T)_{max}$ of 290.2 emu K mol^{-1} at $T = 19.5$ K for **1**. $M(H)$ dependences measured at 4.2 K (Figure 2b) for rehydrated **2** and **1** are identical.

In conclusion, as a result of the dehydration of **1**, we obtained a novel molecular magnet **2**. In comparison to **1**, compound **2** exhibits (i) modified topology, (ii) an increased number of cyano bridges per $[Nb(CN)_8]$ unit, and (iii) Mn^{II} centers of decreased coordination number with trigonal-bipyramidal and tetrahedral geometries. The solid−solid transformation from **1** to **2** reveals the features of topotactic reaction[12] with a clearly defined hydrogen-bonding system $Nb^{IV}{-}CN\cdots O_w\cdots H_2O{-}Mn^{II}$ present prior to the complete removal of H_2O and subsequent formation of the seventh $Nb^{IV}{-}CN{-}Mn^{II}$ linkage. The overall structural changes influence substantially the magnetic behavior of the system: a dramatic increase of the ordering temperature from 25 to 62 K and the appearance of a magnetic hysteresis loop for **2**. These features, together with the complete reversibility between **1** and **2**, point to the magnetic spongelike behavior of **2**.[13] The hydration/dehydration-driven change in T_c previously observed in high-dimensional networks including the cyano-bridged ones[14] is unprecedented for $[Nb(CN)_8]$-based systems and, in general, very rare for $[M(CN)_8]^{3-}$-based (M = Mo, W) compounds.[15]

Acknowledgment. The study has been partially supported by the EC within NoE project MAGMANet (Contract NMP-3-CT-2005-515767).

Supporting Information Available: Structure model of **2** in CIF format, the most important metric parameters, the overall structural views, atom labeling scheme, coordination spheres and connectivity of/between Mn^{II} and Nb^{IV} centers in **2**, the role of noncovalent interaction in the system **1/2**, IR spectra (**1**, **2**, and rehydrated **2**), and powder diffraction pattern of **2** (Figures S1−S7 and Table S1). This material is available free of charge via the Internet at http://pubs.acs.org.

IC801248F

---

(12) For examples, see: (a) Randford, J. D.; Vittal, J. J.; Wu, D. *Angew. Chem., Int. Ed.* **1998**, *37*, 1114–1116. (b) Randford, J. D.; Vittal, J. J; Wu, D.; Yang, X. *Angew. Chem., Int. Ed.* **1999**, *38*, 3498–3501. (c) Nagarathinam, M.; Vittal, J. J. *Angew. Chem., Int. Ed.* **2006**, *45*, 4337–4341. (d) Lesage, J.; Guesdon, A.; Hervieu, M.; Raveau, B. *Chem. Mater.* **2006**, *18*, 2895–2903.

(13) (a) Larionova, J.; Chavan, S. A.; Yakhmi, J. V.; Gulbrandsen Frøystein, A.; Sletten, J.; Sourisseau, C.; Kahn, O. *Inorg. Chem.* **1997**, *36*, 6374–6381. (b) Kahn, O.; Larionova, J.; Yakhmi, J. V. *Chem.—Eur. J.* **1999**, *5*, 3443–3449.

(14) For examples, see: (a) Larionova, J.; Clérac, R.; Sanchiz, J.; Kahn, O.; Golhen, St.; Ouahab, L. *J. Am. Chem. Soc.* **1998**, *120*, 13088–13095. (b) Tanase, St.; Tuna, F.; Guionneau, Ph.; Maris, Th.; Rombaut, G.; Mathonière, C.; Andruh, M.; Kahn, O.; Sutter, J.-P. *Inorg. Chem.* **2003**, *42*, 1625–1631. (c) Kaneko, W.; Ohba, M.; Kitagawa, S. *J. Am. Chem. Soc.* **2007**, *129*, 13706–13712.

(15) (a) Nowicka, B.; Rams, M.; Stadnicka, K.; Sieklucka, B. *Inorg. Chem.* **2007**, *46*, 8123. (b) Ohkoshi, S.-i.; Tsunobuchi, Y.; Takahashi, H.; Hozumi, T.; Shiro, M.; Hashimoto, K. *J. Am. Chem. Soc.* **2007**, *129*, 3084–3085.